

Population Synthesis for Symbiotic X-ray Binaries

G.-L. Lü^{1,2*}, C.-H. Zhu^{1,2}, K. A. Postnov³, L. R. Yungelson⁴, A. G. Kuranov³, N. Wang^{1†}

¹National Astronomical Observatories / Xinjiang Observatory, the Chinese Academy of Sciences, Urumqi, 830011, China

²School of Physical Science and Technology, Xinjiang University, Urumqi, 830046, China

³Sternberg Astronomical Institute, Moscow M.V. Lomonosov State University, 13 Universitetski pr., Moscow, 119991, Russia

⁴Institute of Astronomy of the Russian Academy of Sciences, 48 Pyatnitskaya Str., Moscow, 119017, Russia

ABSTRACT

Symbiotic X-ray binaries (SyXBs) comprise a rare class of low-mass X-ray binaries. We study the Galactic SyXBs, which we consider as detached binaries composed of low-mass giants and wind-fed neutron star companions, by simulation of the interaction of a magnetized neutron star (NS) with its environment and utilizing a population synthesis code. We focus mainly on the parameters that influence observational appearance of the SyXB: the donor wind velocity (v_w) and the angular momentum distribution in the shell of matter settling onto NS. We estimate the birthrate of SyXB as $\sim 4.1 \times 10^{-5} \text{ yr}^{-1}$ to $\sim 6.6 \times 10^{-6} \text{ yr}^{-1}$ and their number in the Galaxy as $\sim (100 - 1000)$. Assumed stellar wind velocity from cool giants is the input parameter that influences the model SyXBs population most.

Among known SyXBs or candidate systems, 4U 1954+31 and IGR J16358-4724 in which NS have very long spin periods may host quasi-spherically accreting NSs. GX 1+4 has a peculiar long-term spin behaviour and it may also be a quasi-spherical wind-accreting source. We cannot identify whether there are wind-fed accretion disks in 4U 1700+24, Sct X-1, IRXS J180431.1-273932 and 2XMM J174016.0-290337.

Key words: binaries: symbiotic—pulsar: general—stars: neutron—X-ray: stars

1 INTRODUCTION

Usually, symbiotic stars are binaries in which a hot white dwarf (WD) component burns hydrogen accreted from a cool giant companion which loses mass via stellar wind or Roche lobe overflow (Tutukov & Yungelson 1976). Theoretical studies of the population of symbiotic stars have been published, e.g., by Han et al. (1995); Yungelson et al. (1995); Iben & Tutukov (1996); Lü et al. (2006, 2008, 2009, 2011).

Recently, a small but rapidly growing subclass of symbiotic stars gained attention, in which accreting component is a neutron star (NS). All these systems are hard X-ray emitters (Mürset et al. 1997). They are low-mass X-ray binaries, with possible exception of Sct X-1 (Kaplan et al. 2007), for which a high-mass solution also is viable. Masetti et al. (2006) dubbed these systems symbiotic X-ray binaries (SyXBs). Currently, 10 binaries are classified as SyXBs or candidate systems (Table 1).

Remarkable features of SyXBs are their orbital periods, among the longest determined for low-mass X-ray binaries (Liu et al. 2007) and long NS spin periods. With a 18300 s

spin period, 4U 1954+31 is the slowest accretion-powered NS known to date (Masetti et al. 2006). Long spin periods of NS in SyXBs are not easy to understand assuming the standard disk accretion. In that case, equilibrium NS spin periods would require magnetar-like magnetic fields of NSs. However, long periods find natural explanations if accretion onto NS proceeds quasi-spherically. The quasi-spherical accretion onto NS was reconsidered in the recent paper by Shakura et al. (2012). It was shown that at small X-ray luminosities, $L_x < 4 \times 10^{36} \text{ erg/s}$, the subsonic settling accretion regime from the stellar wind onto NS takes place, during which an effective removal of angular momentum from the NS magnetosphere can take place through hot convective shell formed above the magnetosphere. In this accretion regime, equilibrium spin periods of NS can be very long even for the standard values of the NS magnetic fields $\sim 10^{12} - 10^{13} \text{ G}$. This theory was applied for explanation of the observed features of low-luminosity X-ray pulsars, including long-term spin-down of NS and spin-luminosity correlations in GX 1+4 (González-Galán et al. 2012), the 5-h spin period of 4U 1954+31 (Marcu et al. 2011), the NS spin and luminosity behaviour in X Per (Lutovinov et al. 2012), etc.

Clearly, the model of the Galactic population of SyXBs needs a detailed treatment of accretion process onto NSs, to

* E-mail: guolianglv@gmail.com (LGL)

† E-mail: na.wang@xao.ac.cn

Table 1. Parameters of observed symbiotic X-ray binaries. Columns 1 to 7 list the name of the star, spin period P_s and its derivative \dot{P}/P_s , orbital period P_{orb} , X-ray luminosity, the distance from the Sun, spectral type of companion to NS. References: C97-Chakrabarty & Roche (1997); B97-Bildsten et al. (1997); H06-Hinkle et al. (2006); G12-González-Galán et al. (2012); C08-Corbet et al. (2008); M06-Masetti et al. (2006); M02-Masetti et al. (2002); K07-Kaplan et al. (2007); M07-Masetti et al. (2007); N07-Nucita et al. (2007); P04-Patel et al. (2004); P07-Patel et al. (2007); B06-Bodaghee et al. (2006); N10-Nespoli et al. (2010); L05-Lutovinov et al. (2005); T06-Thompson et al. (2006); F10-Farrell et al. (2010); M11-Masetti et al. (2011).

SyXB	P_s (s)	\dot{P}_s/P_s	P_{orb} (days)	L_X (erg s $^{-1}$)	Distance(Kpc)	Spectral type
GX 1+4	120 ^(C97)	transition ^(B97)	1161 ^(H06)	10 ³⁵ —10 ³⁶ ^(G12)	4.3 ^(H06)	M5 III ^(C97)
4U 1954+31	~ 18300 ^(C08)	-1.4×10^{-9} ^(C08)	?	$4 \times 10^{32} - 10^{35}$ ^(M06)	1.7 ^(M06)	M4 III ^(M06)
4U 1700+24	?	?	404 ^(M02)	$2 \times 10^{32} - 10^{34}$ ^(K07)	0.42 ^(M06)	M2 III ^(M02)
Sct X-1	113 ^(K07)	3.9×10^{-9} ^(K07)	?	2×10^{34} ^(K07)	≥ 4 ^(K07)	Late K/early M I-III ^(K07)
IGR J16194-2810	?	?	?	$\leq 7 \times 10^{34}$ ^(M07)	≤ 3.7 ^(M07)	M2 III ^(M07)
IRXS J180431.1-273932	494 ^(N07)	?	?	$\leq 6 \times 10^{34}$ ^(N07)	10 ^{(N07)?}	M6 III ^(N07)
IGR J16358-4724	5850 ^(P04)	3.1×10^{-8} ^(P07)	?	$3 \times 10^{32} - 3 \times 10^{36}$ ^(P07)	5-6; 12-13 ^(L05)	K-M III ^(N10)
IGR J16393-4643	912 ^(B06,T06)	1.0×10^{-11} ^(N10)	50.2 ^(N10)	?	~ 10 ^(B06)	K-M III ^(N10)
2XMM J174016.0-290337	626 ^(F10)	?	?	$\sim 3 \times 10^{34}$ ^(F10)	~ 8.5 ^(F10)	K1 III ^(F10)
CGCS 5926	?	?	~ 3000 ^(M11)	?	5 ^(M11)	C ^(M11)

which we pay particular attention in the present paper. We focus on the population synthesis for SyXBs. We simulate zero-age population of NSs with companions and then follow evolution of the population with special accent on the spin and magnetic field of NSs interacting with the matter lost by their companions. In §2 we present our assumptions and describe some details of the modelling algorithm. In §3 we present a detailed example of the evolution of a NS interacting with its companion. In §4 the properties of the model population of SyXBs are presented and individual observed SyXBs are discussed. Conclusions follow in §5.

2 THE MODELS

For the simulation of binary evolution, we use rapid binary star evolution code BSE (Hurley et al. 2002) with updates by Kiel & Hurley (2006). If any input parameter is not specially mentioned, its default value is taken from these papers. The code is extended with an algorithm for the treatment of spin evolution of a magnetized NS, as described in §§2.3, 2.3.1, 2.3.2.

Like in the main case considered in our study of symbiotic stars with white dwarf components (Lü et al. 2006), we use Miller & Scalo (1979) initial mass-function for primary components, a flat distribution of initial mass ratios of components (Kraicheva et al. 1989; Goldberg & Mazeh 1994). We assume that all binaries have initially circular orbits. After a supernova explosion, new parameters of the orbit are derived using standard formulae, (e. g., Hurley et al. 2002).

The model is normalized to formation of one binary with $M_1 \geq 0.8M_\odot$ per year (Yungelson et al. 1993). We use 10^7 binary systems in the Monte-Carlo simulations. This gives a statistical error $\leq 5\%$ for the number of Galactic SyXBs.

Below, we only mention several specific assumptions used in the code.

2.1 Kick Velocity

Nascent NS receive an additional velocity (“kick”) due to a still enigmatic process that violates spherical symmetry during the collapse of a massive star or later. The kicks have dichotomous nature, as it was suggested quite early by Katz (1975) and later confirmed by, e. g., Hartman et al. (1997); Pfahl et al. (2002). Observationally, the kick is not well constrained due to numerous selection effects. Currently, high ($\sim 100 \text{ km s}^{-1}$) kicks are associated with NS originating from core-collapse supernovae, while low kicks ($\sim 10 \text{ km s}^{-1}$) — with NS born in electron-capture supernovae and accretion-induced collapses (see, e. g., Ivanova et al. (2008) for references and discussion).

Following Podsiadlowski et al. (2004), we assume that core collapses are experienced by stars with ZAMS mass $M/M_\odot \geq 11$. For NSs born via core-collapse we apply Maxwellian distribution of kick velocity v_k

$$P(v_k) = \sqrt{\frac{2}{\pi}} \frac{v_k^2}{\sigma_k^3} e^{-v_k^2/2\sigma_k^2}. \quad (1)$$

We use velocity dispersion $\sigma_k = 190 \text{ km s}^{-1}$, which is consistent with the data on pulsar proper motions (Hansen & Phinney 1997). Variation of σ_k between 50 and 200 km s^{-1} , introduces an uncertainty $\lesssim 3$ in the birthrate of low- and intermediate-mass X-ray binaries (Pfahl et al. 2003). Since in this paper we focus on the physical parameters of close binaries that mostly affect observational appearance of NS — their equilibrium spin period and X-ray luminosity, we do not discuss the effects of σ_k on SyXB’s population.

Electron-capture supernovae (ECS) and accretion-induced collapses (AIC) are associated with formation of ONeMg cores of stars or white dwarfs. Collapse is triggered by electron captures on ^{20}Ne and ^{24}Mg (Miyaji et al. 1980). ECS occur in single stars, while AIC in white dwarfs in close binaries. The range of stars that form ONeMg cores or dwarfs depends on subtle details of the treatment of rotation, mass loss, mixing etc. and also depends on stellar evolution code applied (see, e. g., discussion in Podsiadlowski et al. 2004). Following Kiel et al. (2008), we

assume that ECS occurs if stellar helium core mass is $1.4 \leq M_{\text{He}}/M_{\odot} \leq 2.5$. Progenitors of these stars have ZAMS mass between ~ 8.0 and $11.0 M_{\odot}$ (Hurley et al. 2000). Accretion-induced collapses happen when accreting ONeMg WD reach the Chandrasekhar limit. Progenitors of ONeMg WDs have ZAMS mass between ~ 6.3 and $8.0 M_{\odot}$ (Hurley et al. 2000).

Considering the problem of retention of NSs in globular clusters, Pfahl et al. (2002) suggested that NSs born in ECS and AIC have velocity dispersion lower than 50 km s^{-1} . In this study we assume it equal to 20 km s^{-1} .

Response of ONeMg dwarfs to accretion is treated in the same way as for CO WD (see for the details Lü et al. 2009).

2.2 Mass Transfer and Angular Momentum Loss

Mass transfer may occur by accretion of the matter lost via stellar wind or due to Roche-lobe overflow. If the system is detached, we apply Bondi & Hoyle (1944) accretion formula in which mass-accretion rate greatly depends on the wind velocity v_w . Determination of v_w is difficult. According to Harper (1996), the main characteristic of the cool winds of evolved K and early M giants is that their terminal velocities are lower than the surface escape velocity, typically, $v_w \leq 1/2 v_{\text{esc}}$. As the wind velocity is very important parameter for accretion, we set $v_w = 1/2 v_{\text{esc}}$ and $v_w = 2 v_{\text{esc}}$ in different simulations.

For the case of RLOF, the critical issue is whether mass loss occurs on dynamical time scale and common envelope (CE) forms. This depends on the mass ratio of components $q = M_d/M_a$. Following Hurley et al. (2002), we assume that condition for formation of CE (if the accretor is a main-sequence star) is $q > 4$ for the donors in the Hertzsprung gap. If the donor is a giant, critical condition is given by $q > q_{\text{cr}}$, where

$$q_{\text{cr}} = 0.362 + \frac{1}{3 \times (1 - M_c/M)}, \quad (2)$$

where M_c is the mass of the stellar degenerate core (Webbink 1988).

For common envelopes, we apply Webbink (1984) equation for energy balance, as modified by de Kool (1990) by adding a numerical “structure” factor λ , meant to describe the dependence of binding energy of the donor on the density distribution. Then, final separation of the components after CE-stage depends on the product of λ and “common envelope efficiency” α_{ce} (the fraction of binary binding energy which is spent to expell common envelope). We assume $\alpha_{\text{ce}} \times \lambda = 0.5$. Pfahl et al. (2003) have shown that such high value of $\alpha_{\text{ce}} \times \lambda$ is necessary for explanation of the birthrate of Galactic population of LMXB. Reduction of $\alpha_{\text{ce}} \times \lambda$ may result in decrease of the birthrate of SyXB due to increase of the number of mergers.

In the treatment of angular momentum loss we follow original BSE code with only exception: for magnetic braking we replace Eq. (50) of Hurley et al. (2002) by a formula from Verbunt & Zwaan (1981) with $\lambda = 1$ and $k^2 = 0.1^1$.

¹ The reason for this change is the following. Hurley et al. (2002) use a modification of magnetic braking law parametrization suggested by Rappaport et al. (1983). Then, BSE produces a long-

2.3 Evolution of Neutron Stars

The regime of interaction of a rotating magnetized NS (single or in a binary system) with surrounding matter has been recognized to be the most important astrophysical aspect of its evolution, see, e. g., Pringle & Rees (1972); Illarionov & Sunyaev (1975); Ghosh & Lamb (1978, 1979a,b); Lovelace et al. (1995, 1999)). From the point of view of population synthesis, a convenient way of describing NS evolution was elaborated by Lipunov et al. (1992). Progress in the 3D MHD simulations of the interaction of a rotating magnetized NS with accreting plasma generally confirmed the basic ideas (Romanova et al. 2002, 2003, 2004, 2005).

The regime of interaction of a rotating magnetized NS with its environment can be determined by relations between four characteristic radii:

- the radius of the light cylinder $R_l = c/\omega$ where c is the speed of light and ω is the spin frequency of NS;
- the radius of the gravitational capture (the Bondi radius)

$$R_G = \frac{2GM_{\text{NS}}}{v_{\infty}^2},$$

where M_{NS} is the mass of NS and v_{∞} is the velocity of surrounding matter;

- the corotation radius $R_c = (GM/\omega^2)^{1/3}$;
- the radius R_{st} where the flow of accreted matter (free-fall or accretion disk) is stopped due to interaction with the NS magnetosphere.

Depending on the relations between the above four radii, NS can be in several basic evolutionary states (Lipunov et al. 1992):

- Ejector state [$R_{\text{st}} > \max(R_G, R_l)$], in which the pressure of relativistic particle wind is sufficient to keep the stellar wind plasma of the companion away from the NS magnetosphere. For example, ordinary radio pulsars form a subclass of ejectors (additional physical conditions may be required for effective relativistic plasma creation);
- Propeller state [$R_c < R_{\text{st}} < \max(R_G, R_l)$], in which the relativistic wind pressure cannot prevent the infalling matter from interaction with the magnetosphere, while the fast rotating magnetic field prevents the matter from stationary accretion onto the NS surface;
- Accretor state ($R_{\text{st}} < R_c$), in which accretion onto magnetized NS is centrifugally allowed, and the NS magnetic field channels the accreting material toward the magnetic poles of the NS.

We shall assume that R_{st} is equal to the Alfvén radius R_A . For disk and quasi-spherical supersonic accretion (see below)

$$R_A = (\mu^2 / (\dot{M}_{\text{NS}} \sqrt{2GM_{\text{NS}}}))^{2/7}, \quad (3)$$

where \dot{M}_{NS} is the accretion rate onto NS, magnetic dipole moment $\mu = B_{\text{NS}} R_{\text{NS}}^3 / 2$, and B_{NS} and R_{NS} are the magnetic field and the radius of NS, respectively.

However, Eq. (3) is valid only if the accretion rate is

living population of systems with giant donors with mass $\simeq 0.1 M_{\odot}$, contradicting observations.

not too high and the accretion luminosity is below the Eddington limit. For the supercritical accretion via a disk, Shakura & Sunyaev (1973) suggested that the accretion rate in the disk begins to fall monotonically from certain radius $R = R_s$ (the spherization radius). The super-Eddington accretion onto magnetized NSs was studied in detail by Lipunov (1982) and summarized in Lipunov (1987). The spherization radius R_s is approximately given by

$$R_s = \frac{\kappa}{4\pi c} \dot{M}_{\text{NS}},$$

where κ is the opacity of the accreting matter. When \dot{M}_{NS} is higher than the Eddington accretion rate, NSs can accrete via the disk at a rate

$$\dot{M}_{\text{NS}}^{\text{S}} = \frac{R_A}{R_s} \dot{M}_{\text{NS}}.$$

The excess of the matter is expelled in the form of a wind from a supercritical accretion disk and carries away the specific orbital angular momentum of the NS. In the supercritical regime the Alfvén radius is determined as (see Lipunov (1987))

$$R_{\text{SA}} = \left(\frac{\mu^2 \kappa}{4\pi c \sqrt{2GM}} \right)^{2/9}. \quad (4)$$

Similarly, in the case of super-Eddington accretion, depending on the relations between R_i , R_G , R_c , and R_A , NS can be in super-ejector (SE), super-propeller (SP) and super-accretor (SA) states (Lipunov 1987).

For a NS, "evolution" means that its basic parameters which determine the interaction with the surrounding medium change. First of all, this concerns NS spin and magnetic field. The effect of the NS mass increase in the accretion state is generally less important, unless a hypercritical accretion (especially inside common envelopes) is allowed. Then the accretion-induced formation of a black hole may occur (see, e. g., Brown & Lee (2004) for more details).

2.3.1 Spin evolution

Spin evolution (spin-up or spin-down) of a NS in a binary system can be conveniently described by an angular momentum conservation equation

$$\frac{dI\omega}{dt} = K_{\text{su}} - K_{\text{sd}}, \quad (5)$$

where I is NS momentum of inertia, K_{su} and K_{sd} are spin-up and spin-down torques, respectively. Their forms are different in different evolutionary states and also depend on the mode of accretion, i.e., whether accretion disk is present or accretion proceeds quasi-spherically. At small accretion rates, spin evolution of a NS in a binary system proceeds almost identically to that of a single NS, so we neglect interaction with matter for $\dot{M} < 10^{-15} M_{\odot} \text{ yr}^{-1}$ and treat NS spin evolution as in the ejector state.

In the ejector state, $K_{\text{su}} = 0$ and NS spins down due to current braking (Beskin et al. 1993). To within a numerical factor depending on the angle ξ between the spin and magnetic dipole axes, the spin-down torque can be written, using the light-cylinder radius R_l , as $K_{\text{sd}} = 2\mu^2/(3R_l^3)$. The secular change of the angle ξ is beyond the scope of our consideration.

In the propeller state, accretion is centrifugally prohibited, $K_{\text{su}} = 0$, and the spin-down torque can be written using the magnetospheric radius in the form $K_{\text{sd}} = k_t \mu^2/R_A^3$. The numerical factor, k_t is model-dependent but is ~ 1 (Shakura et al. 2012).

In the accretor state, both K_{su} and K_{sd} are determined by the geometry of the accretion flow, as specified below.

Roche lobe overflow. If accretion onto the compact star occurs via Roche lobe overflow through the vicinity of the inner Lagrangian point, an accretion disk is formed². The spin-up torque in both accretor and super-accretor states is determined by the specific angular momentum at the inner disk radius and is $K_{\text{su}} = \dot{M}_{\text{NS}} \sqrt{GM_{\text{NS}} R_A}$. The spin-down torque for disk accretion in the first approximation can be written in all cases using the corotation radius R_c as $K_{\text{sd}} = (1/3)\mu^2/R_c^3$.

The total torque exerted on a NS in the accretor or super-accretor state is then

$$K = \dot{M}_{\text{NS}} \sqrt{GM_{\text{NS}} R_A} - 1/3 \mu^2 R_c^{-3}. \quad (6)$$

The competitive action of spin-up and spin-down torques, on average, diminishes the total torque acting on NS, and an equilibrium state of NS is reached. The equilibrium NS spin period is then (Lipunov & Postnov 1988)

$$P_s^{\text{eq}} = 5.72 M_{\text{NS}}^{-5/7} \dot{M}_{16}^{-3/7} \mu_{30}^{6/7} \text{ s}, \quad (7)$$

where $\mu_{30} = \mu/(10^{30} \text{ G cm}^3)$ is the NS dipole magnetic moment, and $\dot{M}_{16} = \dot{M}_{\text{NS}}/(10^{16} \text{ g/s})$ is the accretion rate.

For super-Eddington accretion, the NS equilibrium period is found to be

$$P_s^{\text{eq}} = 1.76 \times 10^{-1} \mu_{30}^{2/3} M_{\text{NS}}^{-2/3} \text{ s}. \quad (8)$$

Wind-fed accretion. In the wind-fed X-ray binaries, the physical condition for formation of an accretion disk is $j_a > j_K(R_A)$, where $j_a = k_w \Omega_b R_G^2$ is specific angular momentum of the captured stellar wind matter, $\Omega_b = 2\pi/P_{\text{orb}}$ is orbital frequency, k_w is a numerical coefficient, which we set to 0.25 after Illarionov & Sunyaev (1975), $j_K(R_A) = \sqrt{GM_{\text{NS}} R_A}$ is the Keplerian angular momentum at the NS magnetosphere. If an accretion disk forms, the case of wind-fed disk accretion is realized, otherwise, a regime of quasi-spherical accretion is established. We shall assume that the wind-fed disk accretion is similar to the disk accretion via Roche lobe.

As discussed by Shakura et al. (2012), there can be two different regimes of quasi-spherical accretion. First, if the gas heated up in the bow shock cools down rapidly, the matter falls toward NS supersonically. This happens if accretion rate is fairly high (above $\sim 4 \times 10^{16} \text{ g/s}$). In this regime, all gravitationally captured matter eventually reaches the NS surface. Spin evolution of NS is determined by the sign of the specific angular momentum of captured matter, which can be positive (prograde) or negative (retrograde), and NS can spin-up or spin-down, respectively. Numerical simulations (Ho et al. 1989) show that the sign of the specific angular momentum of the captured matter can alternate; here, however, we shall consider only the prograde case,

² Unless the mass-donating component turns out to be inside the magnetosphere of the compact object; this case can be relevant for the accretion onto a magnetized white dwarf, as in AM Her systems

i.e. only NS spin-up during the supersonic accretion with $K_{su} = \dot{M}_{NS} \sqrt{GM} R_A$. To within a factor of 2, the magnetospheric radius R_A in this regime coincides with that for disk accretion [Eq.(3)], and here we shall ignore the difference (but see below).

Second, if accretion rate onto NS is smaller than 4×10^{16} g/s, shocked gas remains hot, a quasi-static extended shell forms around the NS magnetosphere, and accretion proceeds in the subsonic settling regime. In this regime, the actual accretion rate onto NS \dot{M}_{NS} can be lower than the capture rate by NS, and its value is essentially determined by the ability of plasma to enter the NS magnetosphere via instabilities; however, in this paper we shall assume that in this regime all matter captured by the NS from the stellar wind ultimately accretes onto the NS, as in the case of supersonic accretion. This assumption implies that the X-ray luminosity at the model SyXB stage can be higher than in reality, leading to shorter equilibrium NS spin periods. As shown by Shakura et al. (2012), large-scale convective motions set in the shell, and the latter mediates angular momentum transfer to or from the NS magnetosphere depending on X-ray luminosity. The NS spin-up/spin-down equation can be written in the form given by Eq.(5), with the spin-down torque

$$K_{sd} = Z_2 \dot{M}_{NS} \omega R_A^2 \quad (9)$$

and the spin-up torque

$$K_{su} = Z_1 \dot{M}_{NS} \Omega_b R_G^2 \left(\frac{R_A}{R_G} \right)^{2-n}. \quad (10)$$

Here, the dimensionless coefficient Z_1 determines the plasma-magnetosphere coupling and it is a function of the accretion rate \dot{M}_{NS} and NS dipole magnetic moment μ , $Z_2 = Z_1 - 2/3$. The value of the index n reflects different rotational distributions of matter inside the shell ($\omega(R) \sim R^{-n}$); it depends on the treatment of (generally, anisotropic) turbulent viscosity responsible for angular momentum transport in the shell. The analysis of observed X-ray pulsars (Shakura et al. 2012) suggests that an iso-angular momentum distribution with $n = 2$ is most likely, but quasi-Keplerian law with $n = 3/2$ cannot be excluded as well. Therefore, in our modeling we shall consider both quasi-Keplerian ($n = 3/2$) and iso-angular momentum distributions ($n = 2$) as representative cases.

It is important to note that the value of the Alfvén radius itself in the regime of settling accretion is different from that in the case of disk accretion or supersonic quasi-spherical accretion (Eq. (3) above):

$$R_A \approx 10^9 \left(\frac{\mu_{30}^3}{M_{16}} \right)^{2/11} \left(\frac{M_{NS}}{1.5M_\odot} \right)^{-2/11} \text{ cm}. \quad (11)$$

After inserting this expression into the formulae for spin-up/spin-down torques and using the value of Z_1 from Shakura et al. (2012), the NS spin evolution equation reads:

$$I \dot{\omega} = A \dot{M}^{\frac{3+2n}{11}} - B \dot{M}^{3/11}, \quad (12)$$

The accretion-rate independent coefficients A and B are (in CGS units):

$$A \approx 5.33 \times 10^{31} (0.034)^{2-n} K_1 \mu_{30}^{\frac{13-6n}{11}} v_8^{-2n} \times \left(\frac{P_{orb}}{10d} \right)^{-1} \left(\frac{M_{NS}}{1.5M_\odot} \right)^{47/22-13/11(2-n)}, \quad (13)$$

$$B \approx 5.4 \times 10^{32} K_1 \mu_{30}^{\frac{13}{11}} \left(\frac{P_s}{100s} \right)^{-1} \left(\frac{M_{NS}}{1.5M_\odot} \right)^{-5/22}. \quad (14)$$

Here $v_8 = v_w/(1000 \text{ km/s})$ is the relative stellar wind velocity, K_1 is a dimensionless numerical factor which differs for different systems; we shall assume $K_1 = 40$, which is the typical value found from the analysis of observed X-ray pulsars (Shakura et al. 2012).

In the equilibrium state (when the total torque exerted on the NS vanishes, $K_{su} + K_{sd} = 0$), the equilibrium spin period of a NS in the settling accretion state is independent of the source-specific coefficient K_1 and it is given by

$$P_s^{\text{eq}} \approx 1000 \cdot (0.034)^{n-2} \mu_{30}^{\frac{6n}{11}} v_8^{2n} M_{16}^{-\frac{2n}{11}} \times \left(\frac{P_{orb}}{10d} \right) \left(\frac{M_{NS}}{1.5M_\odot} \right)^{13/11(2-n)-26/11} \text{ s}. \quad (15)$$

In our calculations, we take $M_{NS} = 1.5M_\odot$ in Eqs. (11), (13)-(15). Among other factors, this one appears to be known quite well. In all formulae we omit some lengthy factors describing anisotropic turbulence in the quasi-spherical envelope; taking them into account would change the result to within less than 10 per cent.

We also stress that in the free-fall supersonic accretion case which is realized for high X-ray luminosities ($L_x > 4 \times 10^{36}$ erg/s), spin evolution of a NS is entirely determined by the sign of the captured specific angular momentum, and, strictly speaking, the equilibrium period cannot be determined from the mass accretion rate and NS magnetic field only; in real systems the equilibrium state still could be established due to alternating spin-up/spin-down torques in the inhomogeneous stellar wind, but this cannot be taken into account in our simulations. For prograde angular momentum accretion, the NS in this regime will spin-up until the corotation radius will become comparable with the magnetospheric one, $R_A = R_c$, most likely resulting in the transient accretion or propeller regime. Transient sources are beyond the scope of the present paper.

The values of spin-up and spin-down torques exerted on a rotating magnetized NS are summarized in Table 2. The spin evolution of the NS with these torques at each state can be explicitly understood as a tendency to reach an equilibrium period, P_{eq} , which is derived from the condition $K = 0$. Equilibrium periods are also listed in Table 2.

As mentioned in §2.2, mass loss and mass exchange can change the orbital period. In the ejector and propeller states, the matter transferred from the companion is ejected out of binaries. In this work, the ejection of matter is treated as occurring in Jeans mode, i.e. as spherical wind ejection with the specific angular momentum equal to the NS orbital one.

Since overwhelming majority of NS in SyXB form via core-collapses, we set initial spin periods of neutron stars equal to 10 ms (Cordes et al. 2004).

2.3.2 Magnetic field evolution

For the decay of the magnetic field of an accreting NS, a commonly accepted idea does not exist as yet. Bisnovatyi-Kogan & Komberg (1974) suggested that the decay results from the screening of the original magnetic field by the accreted matter. Ruderman (1991) suggested that the decay is due to the crustal motion on the surface of NS.

Table 2. Spin-up K_{su} and spin-down K_{sd} torques acting on the rotating magnetized NS at basic evolutionary states, and the corresponding equilibrium periods derived from the equation $K_{\text{su}} - K_{\text{sd}} = 0$. We use units $\mu_{30} = \frac{\mu}{10^{30} \text{G cm}^3}$, $\dot{M}_{16} = \frac{\dot{M}}{10^{16} \text{g/s}}$, and $R_{\text{A},8} = \frac{R_{\text{A}}}{10^8 \text{cm}}$.

State	K_{su}	K_{sd}	P_{eq}
E	—	$\frac{2}{3} \frac{\mu^2}{R_{\text{A}}^3}$	—
P	—	$k_{\text{v}} \frac{\mu^2}{R_{\text{A}}^3}$	—
A, disk	$\dot{M}_{\text{NS}} \sqrt{GM R_{\text{A}}}$	$\frac{1}{3} \frac{\mu^2}{R_{\text{c}}^3}$	subcritical: $5.72 M_{\text{NS}}^{-5/7} \dot{M}_{16}^{-3/7} \mu_{30}^{6/7} \text{ s}$ supercritical: $1.76 \times 10^{-1} \mu_{30}^{2/3} M_{\text{NS}}^{-2/3} \text{ s}$
A, quasi-sph., supersonic ($\dot{M}_{\text{NS}} \geq 4 \cdot 10^{16} \text{ g/s}$)	$\dot{M}_{\text{NS}} \sqrt{GM R_{\text{A}}}$	—	—
A, quasi-sph., settling ($\dot{M}_{\text{NS}} < 4 \cdot 10^{16} \text{ g/s}$)	$Z_1 \dot{M}_{\text{NS}} \Omega_{\text{b}} R_{\text{G}}^2 \left(\frac{R_{\text{A}}}{R_{\text{G}}}\right)^{2-n}$	$Z_2 \dot{M}_{\text{NS}} \omega R_{\text{A}}^2$	$1000 \cdot (0.034)^{n-2} [\text{s}] \mu_{30}^{6n} v_8^{2n} \dot{M}_{16}^{-\frac{2n}{11}}$ $\times \left(\frac{P_{\text{orb}}}{10\text{d}}\right) \left(\frac{M_{\text{NS}}}{1.5 M_{\odot}}\right)^{13/11(2-n)-26/11} \text{ s}$

Goldreich & Reisenegger (1992) considered decrease of the magnetic field due to Ohmic decay.

From the statistical analysis of 24 binary radio pulsars, van den Heuvel & Bitzaraki (1995) discovered a clear correlation between the magnetic field and the mass accreted by the NS. In our study, we assume that magnetic field depends exponentially on the amount of accreted matter and use the formula suggested by Osłowski et al. (2011):

$$B_{\text{NS}} = (B_{\text{NS}}^{\text{i}} - B_{\text{min}}) \exp\left(-\frac{\Delta M}{M_{\text{B}}}\right) + B_{\text{min}}, \quad (16)$$

where ΔM is accreted mass, M_{B} is magnetic decay mass scale and B_{min} is the minimal magnetic field of NS. We set $M_{\text{B}} = 0.025 M_{\odot}$ and $B_{\text{min}} = 10^8$ Gauss. B_{NS}^{i} is initial magnetic field of NS. We assume that the initial magnetic fields of nascent NS are distributed log-normally (Faucher-Giguère & Kaspi 2006; Popov et al. 2010). The median value and the dispersion of $\log B_{\text{NS}}^{\text{i}}$ are 12 and 1, respectively.

The decay of the magnetic field of a non-accreting NS should be similar to that of an isolated NS. We assume, after Kiel et al. (2008), that magnetic field decays exponentially due to Ohmic decay

$$B_{\text{NS}} = B_{\text{NS}}^{\text{i}} \exp\left(-\frac{t - t_{\text{acc}}}{\tau_{\text{B}}}\right), \quad (17)$$

where t is the age of the NS, τ_{B} is magnetic field decay time scale and t_{acc} is the time which NS has spent accreting matter via Roche lobe overflow. Kiel et al. (2008) have shown that $\tau_{\text{B}} = 2$ Gyr is optimal in their preferred models of Galactic pulsar population. We use this value of τ_{B} in our model.

3 AN EXAMPLE OF NS EVOLUTION

Symbiotic X-ray binaries are wide and faint X-ray systems (Masetti et al. 2006). In this work, binaries composed of a NS and a giant or a giant-like star are considered as SyXBs if they satisfy the following conditions:

- (i) The systems are detached;
- (ii) NSs are in the accretor state.

Revnitsev et al. (2011) suggested that some LMXBs have giant or giant-like donors which fill their Roche lobes, such as GX 13+1 and Cyg X-2. Usually, these giant donors are still very close to the main sequence and have small He cores. In these LMXBs, the X-ray luminosities are very high. Compared to SyXBs, their orbital periods are very short. In order to understand SyXBs, we also discuss these LMXBs. Further, we use notation ‘‘LMXB’’ for the systems in which giant or giant-like donors fill their Roche lobes.

Below, we present a detailed example of the evolution of an accreting magnetized NS in a binary system, as it emerges using the algorithm for spin and magnetic field evolution presented in the previous sections. We start with a binary which consists of a NS and a main-sequence star. At the onset of evolution, the mass of NS is $1.4 M_{\odot}$, its surface magnetic field strength is 5×10^{12} G, and spin period is 0.01 s. Main-sequence star mass is $1.3 M_{\odot}$. Initial orbital period of the system is 400 day. Figure 1 shows evolution of the NS spin period for different input parameters. In Table 3 we present some important physical values for all points marked by letters in the top left ($v_{\text{w}} = 1/2 v_{\text{esc}}$ and $n = 2$) and bottom right ($v_{\text{w}} = 2 v_{\text{esc}}$ and $n = 3/2$) panels in Fig. 1. For $v_{\text{w}} = 1/2 v_{\text{esc}}$ and $n = 2$, the evolution of P_{s} proceeds as follows.

Before point A, the secondary is in the first giant branch (FGB) stage, but does not fill its Roche lobe. Bondi accretion rate of the NS is below $10^{-15} M_{\odot} \text{ yr}^{-1}$. Neutron star evolves like an isolated object. At point A, mass-capture rate by NS exceeds $10^{-15} M_{\odot} \text{ yr}^{-1}$ and NS starts interacting with its environment. At point A, relations $R_{\text{G}} > R_{\text{A}} > R_{\text{c}}$ (See Table 3) and $j_{\text{a}} < j_{\text{K}}(R_{\text{A}})$ hold and NS enters the propeller state of quasi-spherical accretion. While NS evolves through the propeller state from point A to point B, its spin period increases and R_{c} increases. At point B, R_{A} becomes lower than R_{c} , but $\dot{M}_{\text{NS}} < 4 \times 10^{16} \text{ g/s}$. NS enters the quasi-spherical subsonic settling accretion state, after which the

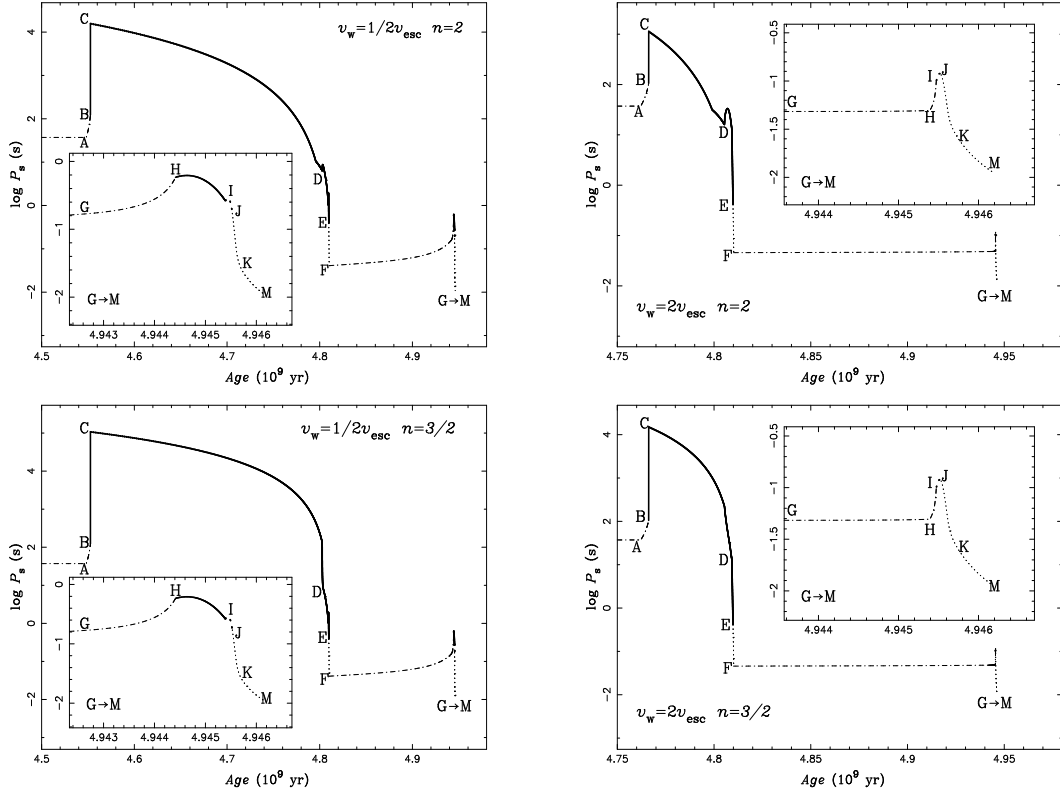


Figure 1. —Spin evolution of an accreting magnetized NS in a binary system for different input parameters. Light dot-dashed lines represent the states in which NS evolves like an isolated NS or it is in the propeller state, that is, the binary does not emit X-rays. Thick solid lines represent the states in which the binary is a SyXB. Thick and thin dotted lines correspond to the states in which the binary is a LMXB and mass accretion rate onto the NS is lower (between points 'I' and 'J') or higher (between 'J' and 'M') than the Eddington critical accretion rate, respectively. In the left two panels, the lines from 'B' to 'E' and from 'H' to 'I' represent the states in which the binary is a SyXB. In the right two panels, the binary is a SyXB between points 'B' and 'E'. The inserts in the panels show detailed evolution between points 'G' and 'M'. See the text and Table 3 for more details.

evolution of P_s is determined by the torque given by Eqs. (10) and (9). The stage of SyXB starts. At the beginning, $K_{sd} > K_{su}$, and the spin period is increasing. With the increase of the spin period, K_{sd} decreases. Soon, at point C, $K_{sd} \sim K_{su}$, the evolution of the spin period is now determined by Eq. (15). With the ascend along FGB, stellar-wind velocity of the giant v_w decreases. This results in the increase of j_a . At point D, $j_a > j_K(R_A)$ and a wind-fed accretion disk forms around NS. After point D, the torque exerted on the NS is given by Eq (6). Due to large P_s and low \dot{M}_{NS} , immediately after point D the spin-up torque is smaller than the spin-down torque, and P_s increases from 6.3 s to 8.7 s. But very soon, with the enhancement of \dot{M}_{NS} and P_s , the spin-up torque becomes larger than the spin-down torque, and P_s starts to decrease.

At point E the secondary overflows its Roche lobe, the system becomes LMXB (in our notation). The mass-accretion rate immediately increases and becomes higher than the Eddington mass-accretion rate. Neutron star becomes a super-accretor.

At point F, the secondary leaves FGB and evolves to the core helium burning stage. Mass-loss rate rapidly decreases, but the velocity of stellar wind is low, so that $j_a > j_K(R_A)$, and neutron star becomes a propeller with a wind-fed ac-

cretion disk. In this state the mater from the disk does not reach the NS due to centrifugal barrier.

At point G, the secondary evolves to the early asymptotic giant branch (E-AGB). With the ascend along AGB, mass-loss rate of the secondary increases. Due to the high mass-accretion rate, spin period P_s rapidly increases. At point H, $R_A \sim R_c$ and $j_a > j_K(R_A)$. The system becomes SyXB with a wind-fed accretion disk. At point I the secondary overflows its Roche lobe, the system becomes LMXB. Very soon, the NS becomes a super-accretor at the point J. At point K the secondary evolves into thermally pulsing asymptotic giant branch star. At point M the secondary leaves AGB.

To summarize, the system is a SyXB between points 'B' and 'E' and 'H' and 'I'. It is a LMXB from point 'E' to point 'F' and from point 'I' to point 'M'.

In our model, in the stages of evolution when the mass-accretion rate onto NS is higher than 4×10^{16} g/s, v_w usually is low, such that $j_a > j_K(R_A)$ and a disk forms. Therefore, the quasi-spherical supersonic accretion hardly occurs in SyXBs.

The case of high wind velocity ($v_w = 2v_{esc}$) and respective spin period evolution are shown in the right panels of Figure 1. High velocity of the stellar wind from the companion to NS results in a low mass-accretion rate by the latter,

Table 3. Some important parameters in the turning points of spin evolution marked by the letters in the top left and bottom right panels of Fig. 1. The 2nd column gives the evolutionary age of the secondary. Columns 3 and 4 give the masses of the NS and the secondary, respectively. The letters in the parentheses in column 4 indicate the evolutionary stage of the secondary: FGB, BHeC, E-AGB and AGB stay for the first giant branch (FGB), core helium burning (BHeC), early asymptotic giant branch (E-AGB), thermally-pulsing asymptotic giant branch (TP-AGB). The radius of the secondary is given in column 5. Columns 6 and 7 list the terminal stellar wind velocity and the mass-accretion rate, respectively. When the secondary overfills Roche lobe, the wind does not play any role. Columns 8, 9, and 10 give the gravitational capture radius R_G , the magnetospheric Alfvén radius R_A and corotation radius R_c , respectively. Column 11 gives the total torque. Columns 12 and 13 show magnetic field and spin period.

Point	Age (10^6 yr)	M_{NS} (M_{\odot})	M_2 (M_{\odot})	R_2 (R_{\odot})	$v_w = 1/2v_{\text{esc}}$		$n = 2$		R_c (cm)	$K_{\text{su}} - K_{\text{sd}}$ (dyn cm)	B_{NS} (G)	P_s (s)
					v_w (km s $^{-1}$)	\dot{M}_{NS} (10^{16} g s $^{-1}$)	R_G (cm)	R_A or R_{SA} (cm)				
A	4548.07	1.40	1.30(FGB)	3.26	194.9	6.5×10^{-6}	2.4×10^{12}	4.2×10^{10}	1.9×10^{10}	-9.0×10^{29}	5.1×10^{11}	37.18
B	4552.66	1.40	1.30(FGB)	3.28	194.3	6.6×10^{-6}	2.4×10^{12}	4.2×10^{10}	4.2×10^{10}	-9.2×10^{29}	5.1×10^{11}	123.1
C	4552.67	1.40	1.30(FGB)	3.28	194.3	6.7×10^{-6}	2.4×10^{12}	4.2×10^{10}	4.2×10^{10}	6.6×10^{30}	5.1×10^{11}	15760
D	4802.68	1.40	1.28(FGB)	38.5	56.4	3.6×10^{-1}	2.6×10^{12}	4.9×10^{10}	5.7×10^{10}	-6.5×10^{31}	5.1×10^{11}	6.328
E	4809.78	1.41	1.21(FGB)	136	—	1.6×10^2	—	2.5×10^7	9.0×10^7	0.0	3.9×10^{11}	0.3927
F	4810.18	1.44	1.16(BHeC)	12.2	94.9	4.5×10^{-3}	1.0×10^{12}	5.1×10^8	2.0×10^7	-1.7×10^{31}	9.7×10^{10}	0.04093
G	4941.68	1.44	1.12(E-AGB)	24.5	66.2	8.7×10^{-2}	2.0×10^{12}	3.0×10^8	4.9×10^7	-8.8×10^{31}	9.7×10^{10}	0.1551
H	4944.42	1.44	1.11(E-AGB)	53.1	44.8	1.9	4.0×10^{12}	1.2×10^8	1.2×10^8	-2.0×10^{32}	9.7×10^{10}	0.5839
I	4945.39	1.44	1.10(E-AGB)	112	—	4.9	—	5.2×10^8	7.0×10^8	0.0	9.2×10^{10}	0.2656
J	4945.53	1.44	1.10(E-AGB)	136	—	1.8×10^2	—	1.3×10^7	5.3×10^7	0.0	8.9×10^{10}	0.1723
K	4945.77	1.47	1.00(TP-AGB)	219	—	5.7×10^3	—	8.9×10^6	1.3×10^7	0.0	3.7×10^{10}	0.0216
M	4946.17	1.49	0.55(TP-AGB)	251	—	2.5×10^3	—	5.4×10^6	8.4×10^6	0.0	1.2×10^{10}	0.001085
Point	Age (10^6 yr)	M_{NS} (M_{\odot})	M_2 (M_{\odot})	R_2 (R_{\odot})	$v_w = 2v_{\text{esc}}$		$n = 3/2$		R_c (cm)	$K_{\text{su}} - K_{\text{sd}}$ (dyn cm)	B_{NS} (G)	P_s (s)
					v_w (km s $^{-1}$)	\dot{M}_{NS} (10^{16} g s $^{-1}$)	R_G (cm)	R_A or R_{SA} (cm)				
A	4762.05	1.40	1.30(FGB)	10.4	436.0	6.4×10^{-6}	7.6×10^{11}	4.0×10^9	1.9×10^9	-8.6×10^{29}	4.6×10^{11}	37.21
B	4766.22	1.40	1.30(FGB)	11.0	423.2	8.4×10^{-6}	8.0×10^{11}	3.8×10^9	3.8×10^9	-1.0×10^{30}	4.6×10^{11}	105.5
C	4766.23	1.40	1.30(FGB)	11.0	423.2	8.4×10^{-6}	8.0×10^{11}	3.8×10^9	3.8×10^9	6.8×10^{30}	4.6×10^{11}	15020
D	4805.38	1.40	1.27(FGB)	51.2	194.8	9.0×10^{-3}	3.3×10^{12}	1.3×10^9	6.2×10^9	1.2×10^{30}	4.6×10^{11}	22.47
E	4809.80	1.40	1.21(FGB)	115	—	6.4×10^1	—	2.6×10^7	9.3×10^7	0.0	4.1×10^{11}	0.4146
F	4810.18	1.44	1.16(BHeC)	12.2	380.0	2.1×10^{-5}	1.0×10^{12}	1.5×10^9	2.2×10^7	-9.9×10^{29}	1.1×10^{11}	0.04572
G	4941.68	1.44	1.13(E-AGB)	24.5	265.0	5.0×10^{-4}	2.0×10^{12}	8.3×10^8	2.2×10^7	-5.6×10^{30}	1.1×10^{11}	0.04807
H	4945.39	1.44	1.11(E-AGB)	113	—	4.9	—	5.8×10^7	2.3×10^7	-1.6×10^{34}	1.1×10^{11}	0.04954
I	4945.47	1.44	1.11(E-AGB)	124	—	2.5×10^1	—	3.7×10^7	3.7×10^7	-6.4×10^{34}	1.1×10^{11}	0.1016
J	4945.53	1.44	1.10(E-AGB)	137	—	1.8×10^2	—	1.4×10^7	4.0×10^7	0.0	1.1×10^{11}	0.1164
K	4945.77	1.46	1.00(TP-AGB)	218	—	5.5×10^3	—	9.6×10^6	1.4×10^7	0.0	4.5×10^{10}	0.02403
M	4946.17	1.49	0.55(TP-AGB)	251	—	2.5×10^3	—	5.7×10^6	8.7×10^6	0.0	1.4×10^{10}	0.01137

which gives a large R_A . As Figure 1 and Table 3 show for the simulation with $v_w = 2v_{\text{esc}}$, at point B of the track when the binary becomes SyXB, the age of the optical star is larger than the one in the simulation with $v_w = 1/2v_{\text{esc}}$. In the $v_w = 2v_{\text{esc}}$ case, the binary never becomes a wind-fed SyXB when the donor is in the AGB stage, but it may become a LMXB for a short time.

In general, $R_A < R_G$ in the accretor state. The spin-up torques in the case of quasi-Keplerian angular momentum distribution in the hot shell at the subsonic accretion state ($n = 3/2$, bottom panels in Fig. 1), are smaller than those in the case of iso-angular momentum distribution ($n = 2$, top panels in Fig. 1). Neutron stars in the bottom panels have longer spin periods at point C. Therefore, the low value of n is favourable to explain SyXBs in which NS have long spin periods.

4 POPULATION OF SYMBIOTIC X-RAY BINARIES

As we mentioned above, theoretical models of the population of LMXBs depend on badly known input parameters,

such as kick velocity and common envelope treatment (e. g., Iben et al. 1995; Pfahl et al. 2003; Zhu et al. 2012). However, in this pioneering study of SyXBs we focus on the effects which are important for the observational appearance of the latter: the donor wind velocity (v_w) and the angular momentum distribution in the shell of matter settling onto NS (index n).

4.1 The Number and Birthrate of the Galactic SyXBs

About 70% (for $v_w = 1/2v_{\text{esc}}$) — 98% (for $v_w = 2v_{\text{esc}}$) of all SyXBs NS are formed via core-collapse, while other $\simeq 30\%$ ($v_w = 1/2v_{\text{esc}}$)— 2% ($v_w = 2v_{\text{esc}}$) via ECS. The reason for negligibly low contribution of post-AIC systems is large initial separation of components which is necessary for formation of an ONeMg WD. The initial orbital periods of the progenitors of SyXBs in which an AIC may happen are the longest. After formation of the WD, the orbit has to remain wide, so that the secondary can evolve to the red giant stage (this means that the efficiency of the common envelope ejection must be high). If the orbit is wide, the ac-

cretion rate is low and unfavourable for AIC. In the systems which produce NS via ECS the primaries usually have ZAMS mass between ~ 8 and $11 M_{\odot}$ and short initial orbital periods. They encounter a common envelope phase when the primaries evolve through HG or FGB. The primaries become naked helium stars and finally form NS. Core-collapse SNe occur in massive stars ($\geq 11 M_{\odot}$) and for progenitors of SyXBs with initially massive primaries the range of initial orbital periods is limited by the possibility of the system to remain bound after SN explosion.

The input parameter n , describing the angular momentum distribution in the hot shell above the NS magnetosphere at the quasi-spherical accretion settling stage, is found to have a negligible effect on SyXBs' birthrate and number. However, the terminal wind velocity v_w greatly influences the birthrate and number of SyXBs and introduces an uncertainty of up to a factor of about 10. The Galactic birthrate and number of SyXB in the simulation with low terminal wind velocity, $v_w = 1/2v_{\text{esc}}$ are $\simeq 4.1 \times 10^{-5} \text{ yr}^{-1}$ and $\simeq 1000$; in the simulation with high terminal wind velocity $v_w = 2v_{\text{esc}}$ they are lower, $\sim 6.6 \times 10^{-6} \text{ yr}^{-1}$ and ~ 100 . Up to now, only 10 SyXBs or candidates were discovered. A possible reason is that SyXBs are difficult to find because of their low X-ray luminosities and transient character of wind accretion.

In contrast to SyXBs, the input parameters n and v_w are found to have a negligible effect on LMXB (semidetached systems in our notation). population. In the simulation with $v_w = 1/2v_{\text{esc}}$, the Galactic birthrate of LMXBs is $\sim 7.0 \times 10^{-5} \text{ yr}^{-1}$, and the number is ~ 10000 . In about 50% of all simulated LMXBs, NS was formed via core-collapse, while in another $\simeq 50\%$ – via ECS. The contribution of post-AIC systems is negligible. Taken at face value, these numbers suggest that LMXBs with giant donors comprise a significant fraction of Galactic LMXBs (cf. Pfahl et al. (2003)). This also means that we encounter the known problem of “overproduction” of LMXBs: while population synthesis codes produce $\sim 10^3 - 10^4$ strong X-ray systems, the number of observed ones is less than 200 (Liu et al. 2006). *Ad hoc* solution, suggested by Pfahl et al. (2003) is possible cyclic behaviour of most LMXB due to irradiation effects, though, self-consistent solution is not available, as yet. However, Büning & Ritter (2004) found that irradiation does not affect giants. The problem remains open.

4.2 Properties of SyXBs

Figure 2 presents, in gray-scale, distributions of the orbital periods P_{orb} of SyXBs and LMXBs vs. masses of their secondary components M_2 . Two upper panels show the population of SyXBs, while two lower panels present LMXBs. The orbital periods of model SyXBs exceed $\simeq 25$ days and extend to $\simeq 30000$ days. The range of orbital periods of the known SyXBs is from 50.2 day (IGR J16393-4643) to 1161 day (GX 1+4). In the distribution for the LMXB population there are two peaks of M_2 and P_{orb} . The upper left peak is due to the systems with long periods in which the secondaries can evolve to the FGB stage and even AGB stage. The peak located lower and to the right is formed mainly by LMXBs in which the secondaries are in the Hertzsprung gap and overflow Roche lobe because of short orbital periods. Comparison of the left and the right panels shows

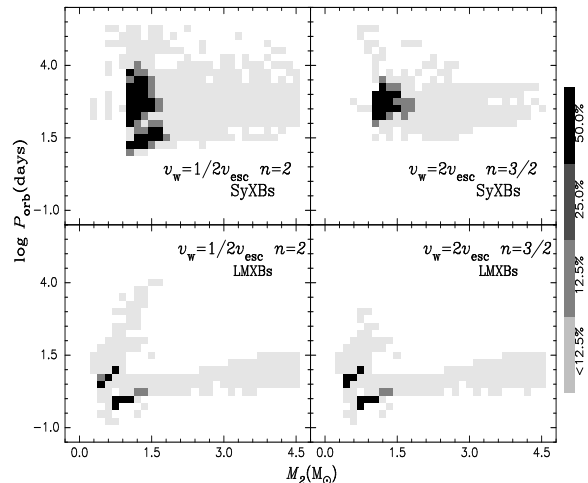


Figure 2. — Distributions of the orbital periods P_{orb} of SyXB and LMXB vs. masses of their secondary stars. Two upper panels are for the SyXBs population, two lower panels for LMXBs population. Gradations of gray-scale correspond to the number density of systems $> 1/2$, $1/2 - 1/4$, $1/4 - 1/8$, $1/8 - 0$ of the maximum of $\frac{\partial^2 N}{\partial \log P_{\text{orb}} \partial \log M_2}$ and blank regions do not contain any stars.

that high wind velocity is unfavourable for formation of the SyXBs and LMXBs with long orbital periods. As Figure 2 shows, SyXBs are predominantly the systems with large M_2 and P_{orb} .

Figure 3 shows the distribution of accretion rates (X-ray luminosities) of NS in SyXBs and LMXB. X-ray luminosities are approximated as

$$L_x = \eta \dot{M} c^2 \simeq 5.7 \times 10^{35} \text{ erg s}^{-1} \left(\frac{\eta}{0.1} \right) \times \left(\frac{\dot{M}}{10^{-10} M_{\odot} \text{ yr}^{-1}} \right), \quad (18)$$

where $\eta \simeq 0.1$ is the efficiency of converting accreted mass into X-ray photons. The peak in the distribution of mass-accretion rates occurs at $\sim 10^{-13} M_{\odot} \text{ yr}^{-1}$, and their X-ray luminosities are between 10^{32} and $10^{36} \text{ erg s}^{-1}$. Therefore, SyXBs are faint X-ray sources. Our results are consistent with observations. LMXBs have high mass-accretion rates ($\sim 10^{-9} M_{\odot} \text{ yr}^{-1}$). In our work, about 1% of LMXBs have super-Eddington accretion.

Figure 4 shows the distributions of spin periods. The range of spin periods in SyXBs is between 0.1 s and $\sim 10^5$ s. In the simulation with $v_w = 2v_{\text{esc}}$ and $n = 3/2$, there are two peaks. The left peak is formed by SyXBs with wind-fed accretion disks, while the right peak is due to quasi-spherically accreting SyXBs because small n is favourable for producing long spin periods. In this simulation, about 20% of SyXBs have wind-fed accretion disks. However, in the simulation with $v_w = 1/2v_{\text{esc}}$ and $n = 2$, only about 7% of SyXBs have wind-fed accretion disks. The low wind velocity results in a high mass-accretion rate which produces shorter spin periods. As the left panel of Fig. 4 shows, there is only one peak which results mainly from quasi-spherically accreting SyXBs. Most of LMXBs have very short spin periods ($\sim 10^{-3}$ s) because NSs have accreted a large amount of matter from their companions. Due to difference in amounts of accreted matter, SyXBs have long spin periods, while LMXBs have very short spin periods. The latter may be good progenitors of binary millisecond pulsars.

Figure 5 shows the distribution of magnetic fields of NSs

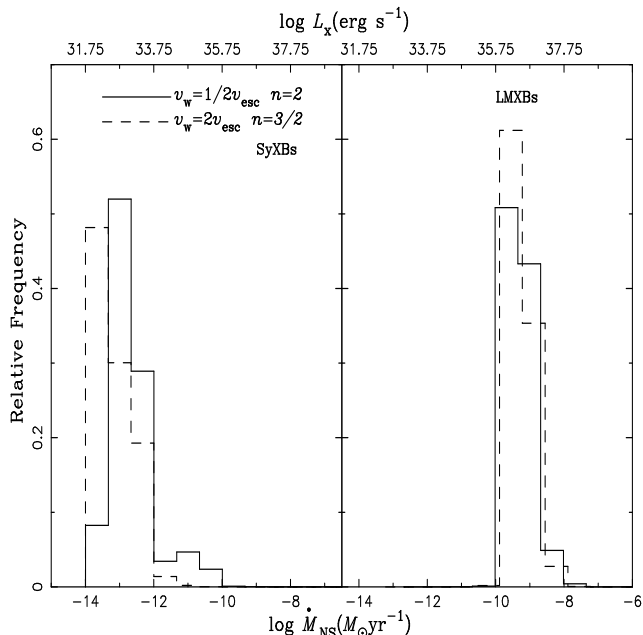


Figure 3. —Distribution of accretion rates (X-ray luminosities) by NSs in SyXBs and LMXBs.

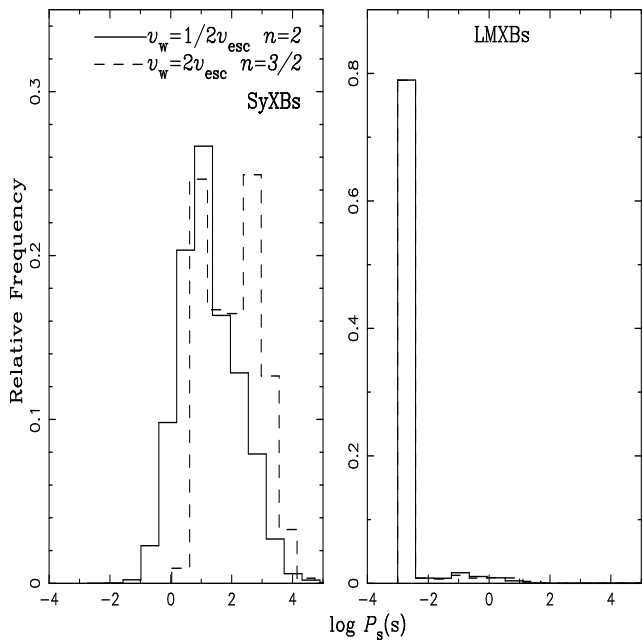


Figure 4. — Number distribution of the spin periods of NSs in SyXBs and LMXBs. The left panel is for population of SyXBs, the right panel is for LMXBs. The numbers are normalized to 1.

in SyXBs and LMXBs. The peak of distribution in SyXBs is at 10^{11} G. The magnetic fields of NSs in SyXBs are not violently suppressed. Most of LMXBs have very weak magnetic fields ($\sim 10^8$ G) because NSs have accreted enough matter to suppress their fields.

4.3 Individual SyXBs

As Table 1 shows, spin periods, orbital periods and X-ray luminosities are the most important parameters of SyXBs.

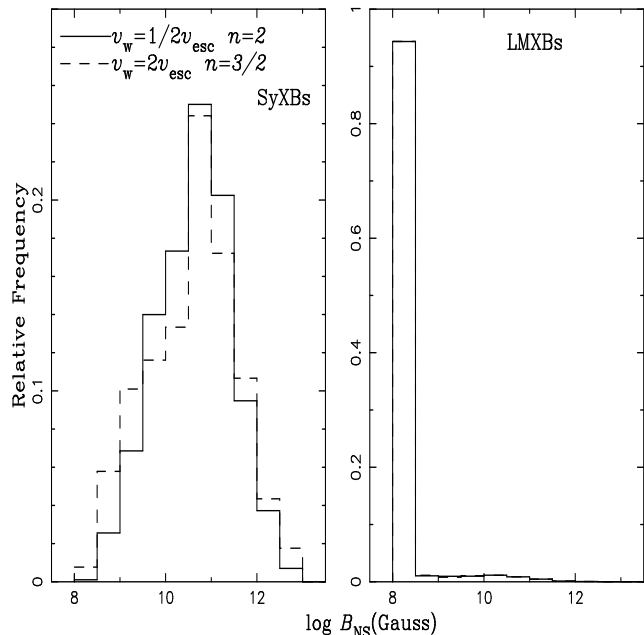


Figure 5. —Similar to Figure 4, but for magnetic fields of NSs in SyXBs and LMXBs.

X-ray luminosities (mass-accretion rates) and spin periods of five SyXBs observed and our results for the sample of SyXBs and LMXBs are plotted in Figure 6. The models with a low wind velocity ($v_w = 1/2 v_{\text{esc}}$) are preferred for explaining the known SyXBs.

Our results in the simulation with $v_w = 1/2 v_{\text{esc}}$ cover the positions of Sct X-1, IRXS J180431.1-273932 and 2XMM J174016.0-290337 very well. Our model cannot identify whether there are accretion disks in these systems. Formation of the disks greatly depends on the wind velocity.

Neutron stars in 4U 1954+31 and IGR J16358-4724 have very long P_s . In order to explain them by the model of a NS with an accretion disk, Patel et al. (2007) suggested that IGR J16358-4724 contains a magnetar. Indeed, as Eqs. (7), (8), and (15) show, the equilibrium NS spin period P_s increases with NS magnetic field. However, the position of 4U 1954+31 and IGR J16358-4724 in Fig. 6 fit well the region occupied by quasi-spherically accreting SyXBs with low wind velocity. Then an ultra-strong magnetic field is not a necessary condition to explain 4U 1954+31 and IGR J16358-4724. The same conclusion was obtained by Marcu et al. (2011) who interpreted the 18300 s pulse period of 4U 1954+31 within the framework of the quasi-spherical accretion model developed by Shakura et al. (2012).

GX 1+4 has a very interesting long-term spin behaviour (González-Galán et al. 2012; Shakura et al. 2012). Based on the properties of an assumed accretion disk around NS, Chakrabarty & Roche (1997) suggested that magnetic field of NS in GX 1+4 should be ultra-strong ($B_{\text{NS}} \sim 10^{14}$ G). Recently, however, based on (Shakura et al. 2012) model, González-Galán et al. (2012) argued that GX 1+4 is not in the disk-accretion state. Instead, the system which currently shows a steady spin-down and can have NS magnetic field close to 10^{13} G, definitely is a quasi-spherical wind-accreting source. As Fig. 6 shows, our result supports the suggestion of González-Galán et al. (2012).

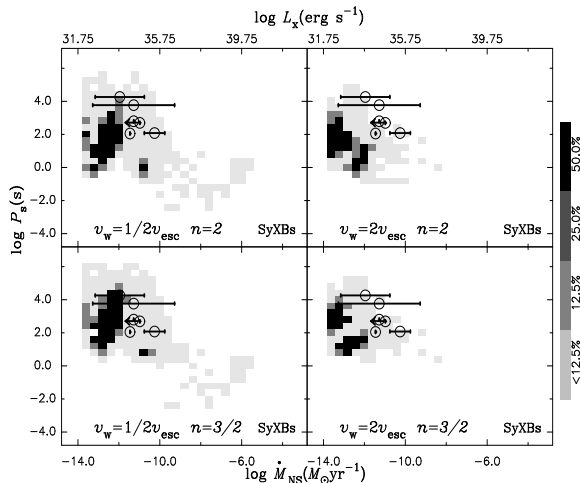


Figure 6. —Gray-scale maps of the distributions of the spin period P_s vs. mass-accretion rate \dot{M}_{NS} (or X-ray luminosity L_x) for SyXBs. The data on observed SyXBs from Table 1 is plotted by cycles.

As seen in Fig. 6, the main population of Galactic SyXB in our population synthesis simulations must have on average lower X-ray luminosities than actually observed. This difference is most likely due to still very approximate treatment of the complicated process of stellar wind accretion onto NS in our model, which ignores temporal variations of the wind properties from cool giants, wind clumping, possible effects of the orbital eccentricity, etc. The settling accretion onto magnetized NSs at small X-ray luminosities can also be unstable (Postnov et al. 2011). However, we stress good correspondence between observed NS spin periods in SyXBs and the ones obtained in quasi-spherical accretion model.

5 CONCLUSIONS

Using simulation of the interaction of magnetized NSs with their environment in binary systems, we investigated Galactic population of SyXBs. In our simulations, the number of Galactic SyXBs is found to be ~ 100 – 1000 , and the estimate of their birthrate is between $\sim 4.1 \times 10^{-5} \text{ yr}^{-1}$ and $\sim 6.6 \times 10^{-6} \text{ yr}^{-1}$. The simulated SyXBs population substantially depends on the properties of the stellar wind velocity from cool giants, which is one of the model input parameters. In our model, SyXBs have found to have wide orbital periods $\sim (10$ – $10000 \text{ days})$, they are faint X-ray sources $\sim (10^{32}$ – $10^{36} \text{ erg s}^{-1})$, and have long spin periods $\sim (0.1$ – $10^5 \text{ s})$.

Our model can explain certain observational properties of some known SyXBs or candidate systems. 4U 1954+31 and IGR J16358-4724, in which NS have very long spin periods, are quasi-spherically accreting SyXBs. In this case an ultra-strong magnetic field is not necessary condition to explain the long spin periods. GX 1+4 also probably is a quasi-spherical wind-accreting source. However, we cannot identify whether there are wind-fed accretion disks in 4U 1700+24, Sct X-1, IRXS J180431.1-273932 and 2XMM J174016.0-290337.

ACKNOWLEDGEMENTS

We acknowledge the referee for constructive suggestions. LGL would like to thank Christopher Tout at the Institute of Astronomy of Cambridge University for his hospitality. This work was supported by the National Natural Science Foundations of China (NSFC) grant 11063002 and 11163005, the Knowledge Innovation Program of the Chinese Academy of Sciences (Grant No. KJCX2-YW-T09), National Basic Research Program of China (973 Program 2009CB824800), Natural Science Foundation of Xinjiang grant 2009211B01 and 2010211B05, and Doctor Foundation of Xinjiang University (BS100106). KAP is supported by RFBR grant 10-02-00951. LRY is supported by RFBR grant 10-02-00231 and the Program of the Praesidium of Russian academy of sciences “Nonstationary processes in the Universe objects”.

REFERENCES

- Beskin V. S., Gurevich A. V., Istomin Y. N., 1993, Physics of the pulsar magnetosphere
- Bildsten L., Chakrabarty D., Chiu J., Finger M. H., Koh D. T., Nelson R. W., Prince T. A., Rubin B. C., Scott D. M., Stollberg M., Vaughan B. A., Wilson C. A., Wilson R. B., 1997, *ApJS*, 113, 367
- Bisnovatyi-Kogan G. S., Komberg B. V., 1974, *Astron. Zh.*, 51, 373
- Bodaghee A., Walter R., Zurita Heras J. A., Bird A. J., Courvoisier T., Malizia A., Terrier R., Ubertini P., 2006, *A&A*, 447, 1027
- Bondi H., Hoyle F., 1944, *MNRAS*, 104, 273
- Brown G. E., Lee C., 2004, *NewA*, 9, 225
- Büning A., Ritter H., 2004, *A&A*, 423, 281
- Chakrabarty D., Roche P., 1997, *ApJ*, 489, 254
- Corbet R. H. D., Sokoloski J. L., Mukai K., Markwardt C. B., Tueller J., 2008, *ApJ*, 675, 1424
- Cordes J. M., Kramer M., Lazio T. J. W., Stappers B. W., Backer D. C., Johnston S., 2004, *New Astronomy Review*, 48, 1413
- de Kool M., 1990, *ApJ*, 358, 189
- Farrell S. A., Gosling A. J., Webb N. A., Barret D., Rosen S. R., Sakano M., Pancrazi B., 2010, *A&A*, 523, A50+
- Faucher-Giguère C.-A., Kaspi V. M., 2006, *ApJ*, 643, 332
- Ghosh P., Lamb F. K., 1978, *ApJL*, 223, L83
- Ghosh P., Lamb F. K., 1979a, *ApJ*, 232, 259
- Ghosh P., Lamb F. K., 1979b, *ApJ*, 234, 296
- Goldberg D., Mazeh T., 1994, *A&A*, 282, 801
- Goldreich P., Reisenegger A., 1992, *ApJ*, 395, 250
- González-Galán A., Kuulkers E., Kretschmar P., Larsson S., Postnov K., Kochetkova A., Finger M. H., 2012, *A&A*, 537, A66
- Han Z., Podsiadlowski P., Eggleton P. P., 1995, *MNRAS*, 272, 800
- Hansen B. M. S., Phinney E. S., 1997, *MNRAS*, 291, 569
- Harper G., 1996, in R. Pallavicini & A. K. Dupree ed., *Cool Stars, Stellar Systems, and the Sun Vol. 109 of Astronomical Society of the Pacific Conference Series, Mass loss and winds from cool giants*. p. 481
- Hartman J. W., Bhattacharya D., Wijers R., Verbunt F., 1997, *A&A*, 322, 477
- Hinkle K. H., Fekel F. C., Joyce R. R., Wood P. R., Smith V. V., Lebzelter T., 2006, *ApJ*, 641, 479

- Ho C., Taam R. E., Fryxell B. A., Matsuda T., Koide H., 1989, *MNRAS*, 238, 1447
- Hurley J. R., Pols O. R., Tout C. A., 2000, *MNRAS*, 315, 543
- Hurley J. R., Tout C. A., Pols O. R., 2002, *MNRAS*, 329, 897
- Iben Jr. I., Tutukov A. V., 1996, *ApJS*, 105, 145
- Iben Jr. I., Tutukov A. V., Yungelson L. R., 1995, *ApJS*, 100, 233
- Illarionov A. F., Sunyaev R. A., 1975, *A&A*, 39, 185
- Ivanova N., Heinke C. O., Rasio F. A., Belczynski K., Fregeau J. M., 2008, *MNRAS*, 386, 553
- Kaplan D. L., Levine A. M., Chakrabarty D., Morgan E. H., Erb D. K., Gaensler B. M., Moon D., Cameron P. B., 2007, *ApJ*, 661, 437
- Katz J. I., 1975, *Nat*, 253, 698
- Kiel P. D., Hurley J. R., 2006, *MNRAS*, 369, 1152
- Kiel P. D., Hurley J. R., Bailes M., Murray J. R., 2008, *MNRAS*, 388, 393
- Kraicheva Z. T., Popova E. I., Tutukov A. V., Yungelson L. R., 1989, *Astrophysics*, 30, 323
- Lipunov V. M., 1982, *Soviet Astronomy*, 26, 54
- Lipunov V. M., 1987, *Ap&SS*, 132, 1
- Lipunov V. M., Börner G., Wadhwa R. S., 1992, *Astrophysics of Neutron Stars*
- Lipunov V. M., Postnov K. A., 1988, *Ap&SS*, 145, 1
- Liu Q. Z., van Paradijs J., van den Heuvel E. P. J., 2006, *A&A*, 455, 1165
- Liu Q. Z., van Paradijs J., van den Heuvel E. P. J., 2007, *A&A*, 469, 807
- Lovelace R. V. E., Romanova M. M., Bisnovatyi-Kogan G. S., 1995, *MNRAS*, 275, 244
- Lovelace R. V. E., Romanova M. M., Bisnovatyi-Kogan G. S., 1999, *ApJ*, 514, 368
- Lü G., Yungelson L., Han Z., 2006, *MNRAS*, 372, 1389
- Lü G., Zhu C., Han Z., Wang Z., 2008, *ApJ*, 683, 990
- Lü G., Zhu C., Wang Z., Huo W., Yang Y., 2011, *MNRAS*, 413, L11
- Lü G., Zhu C., Wang Z., Wang N., 2009, *MNRAS*, 396, 1086
- Lutovinov A., Revnivtsev M., Gilfanov M., Shtykovskiy P., Molkov S., Sunyaev R., 2005, *A&A*, 444, 821
- Lutovinov A., Tsygankov S., Chernyakova M., 2012, *ArXiv e-prints*
- Marcu D. M., Füst F., Pottschmidt K., Grinberg V., Müller S., Wilms J., Postnov K. A., Corbet R. H. D., Markwardt C. B., Cadolle Bel M., 2011, *ApJL*, 742, L11
- Masetti N., Dal Fiume D., Cusumano G., Amati L., Bartolini C., Del Sordo S., Frontera F., Guarnieri A., Orlandini M., Palazzi E., Parmar A. N., Piccioni A., Santangelo A., 2002, *A&A*, 382, 104
- Masetti N., Landi R., Pretorius M. L., Sguera V., Bird A. J., Perri M., Charles P. A., Kennea J. A., Malizia A., Ubertini P., 2007, *A&A*, 470, 331
- Masetti N., Munari U., Henden A. A., Page K. L., Osborne J. P., Starrfield S., 2011, *ArXiv e-prints*
- Masetti N., Orlandini M., Palazzi E., Amati L., Frontera F., 2006, *A&A*, 453, 295
- Miller G. E., Scalo J. M., 1979, *ApJS*, 41, 513
- Miyaji S., Nomoto K., Yokoi K., Sugimoto D., 1980, *PASJ*, 32, 303
- Mürset U., Wolff B., Jordan S., 1997, *A&A*, 319, 201
- Nespoli E., Fabregat J., Mennickent R. E., 2010, *A&A*, 516, A94+
- Nucita A. A., Carpano S., Guainazzi M., 2007, *A&A*, 474, L1
- Ośłowski S., Bulik T., Gondek-Rosińska D., Belczyński K., 2011, *MNRAS*, pp 103–+
- Patel S. K., Kouveliotou C., Tennant A., Woods P. M., King A., Finger M. H., Ubertini P., Winkler C., Courvoisier T., van der Klis M., Wachter S., Gaensler B. M., Phillips C. J., 2004, *ApJL*, 602, L45
- Patel S. K., Zurita J., Del Santo M., Finger M., Kouveliotou C., Eichler D., Göğüş E., Ubertini P., Walter R., Woods P., Wilson C. A., Wachter S., Bazzano A., 2007, *ApJ*, 657, 994
- Pfahl E., Rappaport S., Podsiadlowski P., 2002, *ApJ*, 573, 283
- Pfahl E., Rappaport S., Podsiadlowski P., 2003, *ApJ*, 597, 1036
- Podsiadlowski P., Langer N., Poelarends A. J. T., Rappaport S., Heger A., Pfahl E., 2004, *ApJ*, 612, 1044
- Popov S. B., Pons J. A., Miralles J. A., Boldin P. A., Posselt B., 2010, *MNRAS*, 401, 2675
- Postnov K., Shakura N., Kochetkova A., Hjalmarsdotter L., 2011, *ArXiv e-prints*
- Pringle J. E., Rees M. J., 1972, *A&A*, 21, 1
- Rappaport S., Verbunt F., Joss P. C., 1983, *ApJ*, 275, 713
- Revnivtsev M., Postnov K., Kuranov A., Ritter H., 2011, *A&A*, 526, A94+
- Romanova M. M., Ustyugova G. V., Koldoba A. V., Lovelace R. V. E., 2002, *ApJ*, 578, 420
- Romanova M. M., Ustyugova G. V., Koldoba A. V., Lovelace R. V. E., 2004, *ApJL*, 616, L151
- Romanova M. M., Ustyugova G. V., Koldoba A. V., Lovelace R. V. E., 2005, *ApJL*, 635, L165
- Romanova M. M., Ustyugova G. V., Koldoba A. V., Wick J. V., Lovelace R. V. E., 2003, *ApJ*, 595, 1009
- Ruderman M., 1991, *ApJ*, 366, 261
- Shakura N., Postnov K., Kochetkova A., Hjalmarsdotter L., 2012, *MNRAS*, 420, 216
- Shakura N. I., Sunyaev R. A., 1973, *A&A*, 24, 337
- Thompson T. W. J., Tomsick J. A., Rothschild R. E., in't Zand J. J. M., Walter R., 2006, *ApJ*, 649, 373
- Tutukov A. V., Yungelson L. R., 1976, *Astrophysics*, 12, 521
- van den Heuvel E. P. J., Bitzaraki O., 1995, *A&A*, 297, L41+
- Verbunt F., Zwaan C., 1981, *A&A*, 100, L7
- Webbink R. F., 1984, *ApJ*, 277, 355
- Webbink R. F., 1988, in Mikolajewska, J., Friedjung, M., Kenyon, S. J., & Viotti, R. ed., *The Symbiotic Phenomenon*, Proceedings of IAU Colloq. 103, held in Torun, Poland, 18-20 August, 1987 (ASSL 145). The Formation and Evolution of Symbiotic Stars. Kluwer Academic Publishers, Dordrecht, p. 311
- Yungelson L., Livio M., Tutukov A., Kenyon S. J., 1995, *ApJ*, 447, 656
- Yungelson L. R., Tutukov A. V., Livio M., 1993, *ApJ*, 418, 794
- Zhu C., Lü G., Wang Z., Wang N., 2012, *PASP*, 124, 195

This paper has been typeset from a \TeX / \LaTeX file prepared by the author.